



ARL-TR-7462 • SEP 2015



Optimization of a Circularly Polarized Patch Antenna for Two Frequency Bands

by Jahin S Habib

Approved for public release; distribution is unlimited.

NOTICES

Disclaimers

The findings in this report are not to be construed as an official Department of the Army position unless so designated by other authorized documents.

Citation of manufacturer's or trade names does not constitute an official endorsement or approval of the use thereof.

Destroy this report when it is no longer needed. Do not return it to the originator.



Optimization of a Circularly Polarized Patch Antenna for Two Frequency Bands

by Jahin S Habib

Sensors and Electron Devices Directorate, ARL

REPORT DOCUMENTATION PAGE

Form Approved
OMB No. 0704-0188

Public reporting burden for this collection of information is estimated to average 1 hour per response, including the time for reviewing instructions, searching existing data sources, gathering and maintaining the data needed, and completing and reviewing the collection information. Send comments regarding this burden estimate or any other aspect of this collection of information, including suggestions for reducing the burden, to Department of Defense, Washington Headquarters Services, Directorate for Information Operations and Reports (0704-0188), 1215 Jefferson Davis Highway, Suite 1204, Arlington, VA 22202-4302. Respondents should be aware that notwithstanding any other provision of law, no person shall be subject to any penalty for failing to comply with a collection of information if it does not display a currently valid OMB control number.

PLEASE DO NOT RETURN YOUR FORM TO THE ABOVE ADDRESS.

1. REPORT DATE (DD-MM-YYYY) Sep 2015		2. REPORT TYPE Final		3. DATES COVERED (From - To)	
4. TITLE AND SUBTITLE Optimization of a Circularly Polarized Patch Antenna for Two Frequency Bands				5a. CONTRACT NUMBER	
				5b. GRANT NUMBER	
				5c. PROGRAM ELEMENT NUMBER	
6. AUTHOR(S) Jahin S Habib				5d. PROJECT NUMBER	
				5e. TASK NUMBER	
				5f. WORK UNIT NUMBER	
7. PERFORMING ORGANIZATION NAME(S) AND ADDRESS(ES) US Army Research Laboratory ATTN: RDRL-SER-M 2800 Powder Mill Road Adelphi, MD 20783-1138				8. PERFORMING ORGANIZATION REPORT NUMBER ARL-TR-7462	
9. SPONSORING/MONITORING AGENCY NAME(S) AND ADDRESS(ES)				10. SPONSOR/MONITOR'S ACRONYM(S)	
				11. SPONSOR/MONITOR'S REPORT NUMBER(S)	
12. DISTRIBUTION/AVAILABILITY STATEMENT Approved for public release; distribution is unlimited.					
13. SUPPLEMENTARY NOTES					
14. ABSTRACT The objective of this project is to gain a better understanding of the various techniques that can be used to improve the performance of a circularly polarized microstrip patch antenna. These adjustments include tuning the feed point along different positions on the surface of the patch, analyzing assorted dielectric materials with differing dielectric constants, and optimizing the axial ratio based on the geometry of a circularly polarized patch. Testing the feed point in various locations on the patch allows the designer to improve the S11 and radiation pattern—a peak broadside polar radiation plot is anticipated for optimum performance. Using a high permittivity dielectric lowers the resonant frequency of the patch, allowing the designer to shrink the size of the patch. Altering the patch geometry and optimizing the axial ratio by using a “notching” technique allows the designer to choose from multiple polarization types. With empirical simulations via the High Frequency Structural Simulator (HFSS), expanding this idea for future research will result in producing a scalable multiband microstrip antenna.					
15. SUBJECT TERMS Patch Antenna, Circular Polarization					
16. SECURITY CLASSIFICATION OF:			17. LIMITATION OF ABSTRACT UU	18. NUMBER OF PAGES 36	19a. NAME OF RESPONSIBLE PERSON Gregory A Mitchell
a. REPORT Unclassified	b. ABSTRACT Unclassified	c. THIS PAGE Unclassified			19b. TELEPHONE NUMBER (Include area code) 301-394-2322

Contents

List of Figures	iv
List of Tables	v
Acknowledgments	vii
Student Bio	ix
1. Introduction/Background	1
1.1 Frequency Ranges	1
1.2 Basic Patch Antenna Design	1
1.3 Dielectric Materials	2
1.4 Circular Polarization	2
2. Experiment and Calculations	5
2.1 Patch on Rogers 5870	8
2.2 Patch Rogers 6010	14
3. Results and Discussion	20
4. Future Work	20
5. References	23
Distribution List	26

List of Figures

Fig. 1	Linear polarization vs. CP.....	3
Fig. 2	SF = 0.....	3
Fig. 3	SF = 0.25.....	4
Fig. 4	SF = 0.75.....	4
Fig. 5	SF = 1.25.....	5
Fig. 6	Transverse plane (XY plane) of patch	6
Fig. 7	Normal (YZ) plane of patch antenna	7
Fig. 8	HFSS patch antenna model, 3-dimensional view	7
Fig. 9	Return loss for varying feed points in Rogers 5870. Best S11 curve corresponds to $C_y = 2$ mm.....	9
Fig. 10	Probe 2 mm away from center position, which corresponds to a 9.26-GHz frequency	10
Fig. 11	Return loss for varying SF in Rogers 5870.....	11
Fig. 12	SF = 0.46 on Rogers 5870 substrate with feed point 2 mm from center position.....	12
Fig. 13	Axial ratio for the best SF—corresponds to 9.35 GHz with an optimal axial ratio of 1.11 dB	13
Fig. 14	Radiation plot at 9.35 GHz for optimal axial ratio. Boresight pattern with a 6.19-dB gain.....	14
Fig. 15	Return loss for varying feed points in Rogers 6010. Best S11 curve corresponds to $C_y=2.4$ mm.	15
Fig. 16	Probe 2.4 mm away from center position, which corresponds to a 2.83-GHz frequency	16
Fig. 17	Return loss for varying SF in Rogers 6010.....	17
Fig. 18	SF = 0.21 on Rogers 6010 substrate with feed point 2.4 mm from center position.....	18
Fig. 19	Rogers 6010 axial ratio for the best SF—corresponds to 2.83 GHz with an optimal axial ratio of 1.61 dB	19
Fig. 20	Rogers 6010 radiation plot at 2.83 GHz for optimal axial ratio. Boresight pattern with a 4.62-dB gain.	20
Fig. 21	Transverse (XY) plane of the proposed dual-band antenna design	21
Fig. 22	HFSS model of the dual-band antenna, 3-dimensional view.....	22

List of Tables

Table 1	Variable list for Rogers 5870.....	8
Table 2	Variable list for Rogers 6010.....	8

INTENTIONALLY LEFT BLANK.

Acknowledgments

I would like to thank my mentor, Gregory Mitchell, for his continuous support, motivation, and knowledge for my project this summer. I would also like to thank Theodore Anthony and Dr Amir Zaghoul for their countless hours of teaching and advice.

INTENTIONALLY LEFT BLANK.

Student Bio

Jahin Habib is a rising senior at Virginia Polytechnic Institute and State University (Virginia Tech), majoring in electrical engineering. She was able to research autonomous vehicles at Virginia Tech during the summer of 2013. Recently, she gained valuable hands-on experience at United Technologies Corporation as an electronics engineering intern during the summer of 2014. Working there greatly influenced her toward a path in electromagnetic fields.

Throughout her time at Virginia Tech, Habib has remained involved in a variety of organizations. She is currently a student ambassador for the Bradley Department of Electrical and Computer Engineering and will be serving as president for Virginia Tech's IEEE Student Branch this upcoming school year.

INTENTIONALLY LEFT BLANK.

1. Introduction/Background

Patch antennas gained popularity in the 1970s as advancements in size and performance became useful in communication systems. Compared to its predecessors, such as traditional parabolic reflectors and large-scale antennas, the flat shape and reduced weight of the patch antenna allowed for great flexibility in various space and airborne applications. The use of dielectric materials to further reduce the size of the antenna has allowed technological advancements in global positioning system (GPS) and other wireless devices.¹ Recently, studies on dual-band antennas have emerged to eliminate the restriction on using just 1 frequency band. Empirical work via the High Frequency Structural Simulator (HFSS) has allowed engineers to create scalable multiband microstrip antennas. Several factors were taken into consideration when creating a dual-band antenna to ensure optimal performance in this study. These factors include optimizing the patch length, adjusting the feed point along the patch, varying the height of the dielectric substrates, and using a “notching” technique to incorporate circular polarization (CP).

1.1 Frequency Ranges

When comparing X- and S-band ranges, many differences can be noted as the 2 operate at special frequencies and have variations in their respective parameters. While the X-band operates at 8–12 GHz, the S-band operates at 2–4 GHz in radar engineering. Due to the shorter wavelengths, which, in turn, allow for high resolution imagery, the antennas operating at X-band are small and very portable. On the other hand, antennas operating at the S-band are larger in size. The motivation behind creating a dual-band antenna came from the idea of eliminating the restriction of picking just 1 frequency band, and instead, combining the 2 to form a single element.

1.2 Basic Patch Antenna Design

The patch antenna, also known as the microstrip antenna, is commonly used at frequencies greater than 1 GHz (microwave frequencies). The most common configurations of patch antennas are found in square, rectangular, or circular shapes made out of conductive material. They are approximately $\lambda/2$ in size and placed a small fraction above the ground plane with dielectric material in between. The electrical half-wavelength length of the patch also includes the shortening effect of the material’s dielectric constant (ϵ_r), as follows

$$L = \frac{\lambda_0}{2\sqrt{\epsilon_r}} \quad (1)$$

These low volume and lightweight devices are highly advantageous as the flat structure permits a large aperture with a corresponding high gain value. Their 2-dimensional structure allows for manipulation to fit different applications.³ Once it is tuned to the operating frequency, the patch will achieve maximum radiation efficiency, which is normal to the plane of the patch. A coaxial probe will be used in this study to feed the microstrip antenna; the inner conductor of the coaxial cable is shorted to the patch while the outer conductor is attached to the ground plane.

1.3 Dielectric Materials

As ϵ_r increases, the frequency at which the patch resonates at will decrease, and vice versa. Thinner substrates demonstrate benefits as they minimize excessive radiation and coupling due to the tightly bound fields.² In this study of the CP patch antenna, the X-band element will include a patch and ground plane separated by Rogers 5870 dielectric with $\epsilon_r=2.33$. The S-band will include a patch and ground plane separated by Rogers 6010 dielectric with $\epsilon_r=10.2$.

1.4 Circular Polarization

Antennas that are linearly polarized can transmit and receive linearly polarized signals. Consider a telephone pole that sends out and receives messages. In order for the receiving pole to obtain a vertically polarized signal, the transmitting pole must send out a signal that is vertically polarized. If the receiving pole is horizontally polarized and the transmitting pole is vertically polarized, the message will not convey. CP enables the use of both horizontal and vertical antennas for receiving, as the polarization continuously rotates during transmission. The CP wave does not experience any changes other than a change in direction in a rotational manner. In Fig. 1, we see that the electric-field vector produces a circle in the XY plane.

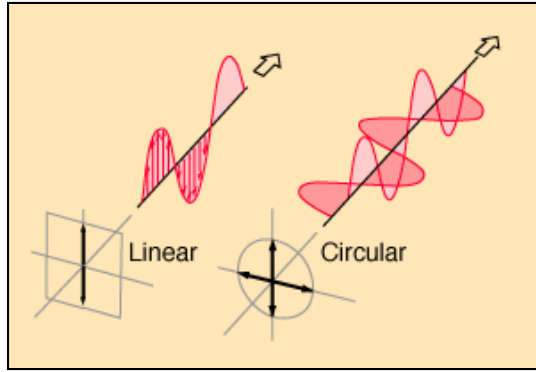


Fig. 1 Linear polarization vs. CP

The square and circular shaped patch antennas discussed thus far radiate linearly polarized waves. Modifications can be made on these elements to obtain CP. One of the methods include trimming the opposite corners of the patch, also known as the notching technique, to create diagonal resonances, which then leads to degeneration. As a result, this allows the antenna to radiate a CP wave. In this study, we used the following formula to solve for the notching value by applying a scaling factor (SF) to the patch.

$$\text{Notching Value} = \frac{L}{2}(1 - \text{SF}) \quad (2)$$

In Figs. 2 through 5, it can be seen that as SF increases, the size of the notch at each corner increases as well.

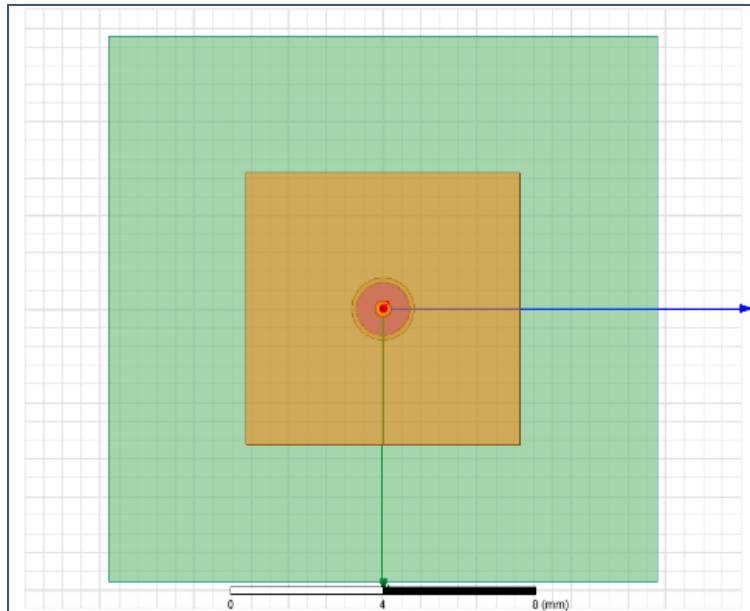


Fig. 2 SF = 0

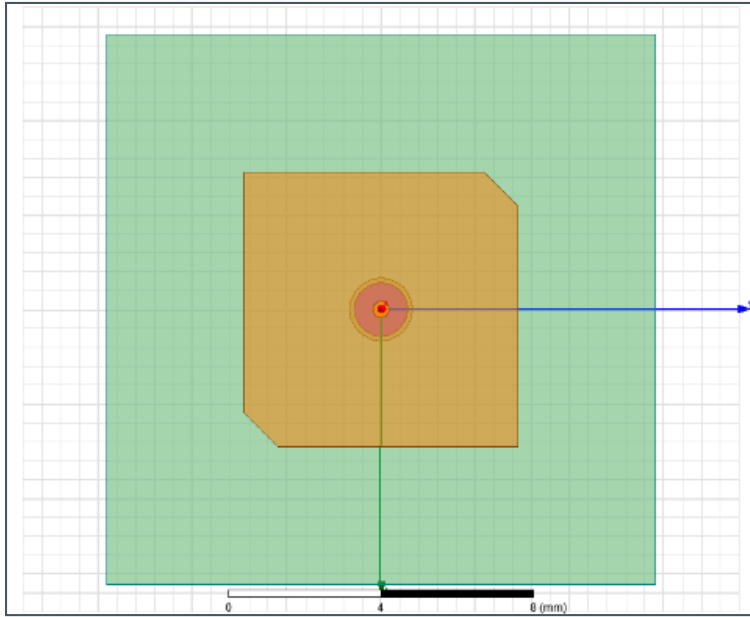


Fig. 3 SF = 0.25

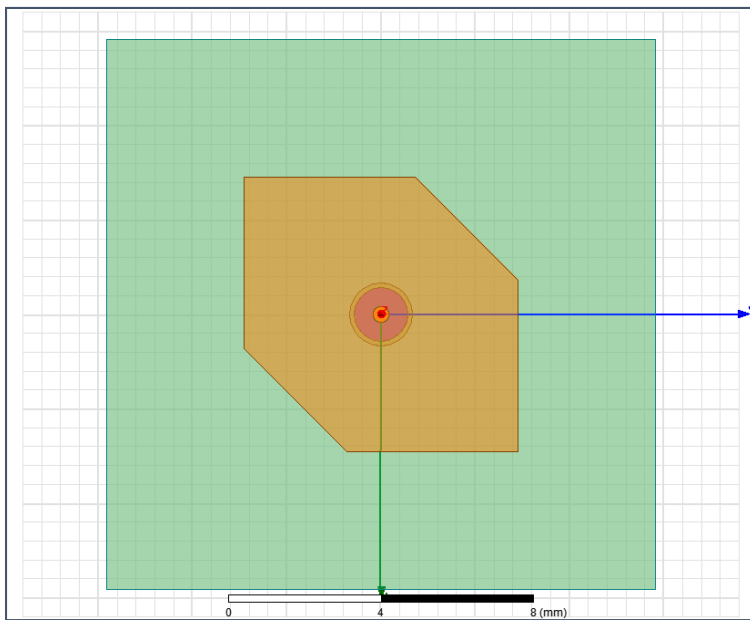


Fig. 4 SF = 0.75

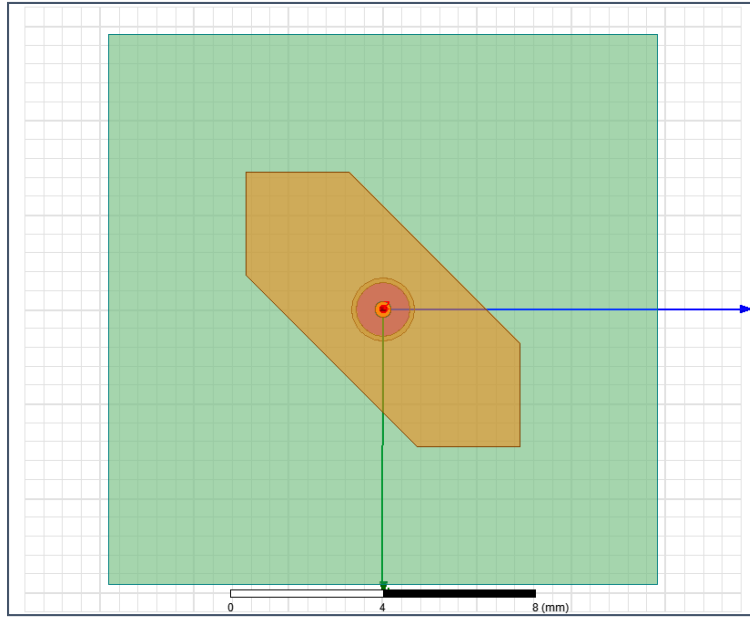


Fig. 5 SF = 1.25

2. Experiment and Calculations

For simulation purposes, the 2 patches with varying dielectric materials were tested separately for initial comparison. Figures 6 through 8 exhibit the variables used in this study to calculate the various antenna parameters. The coaxial probe, which acts as a feed point, is designed to have a 50- Ω impedance. The variable list is shown in Tables 1 and 2 for the S-band patch and the X-band patch, respectively.

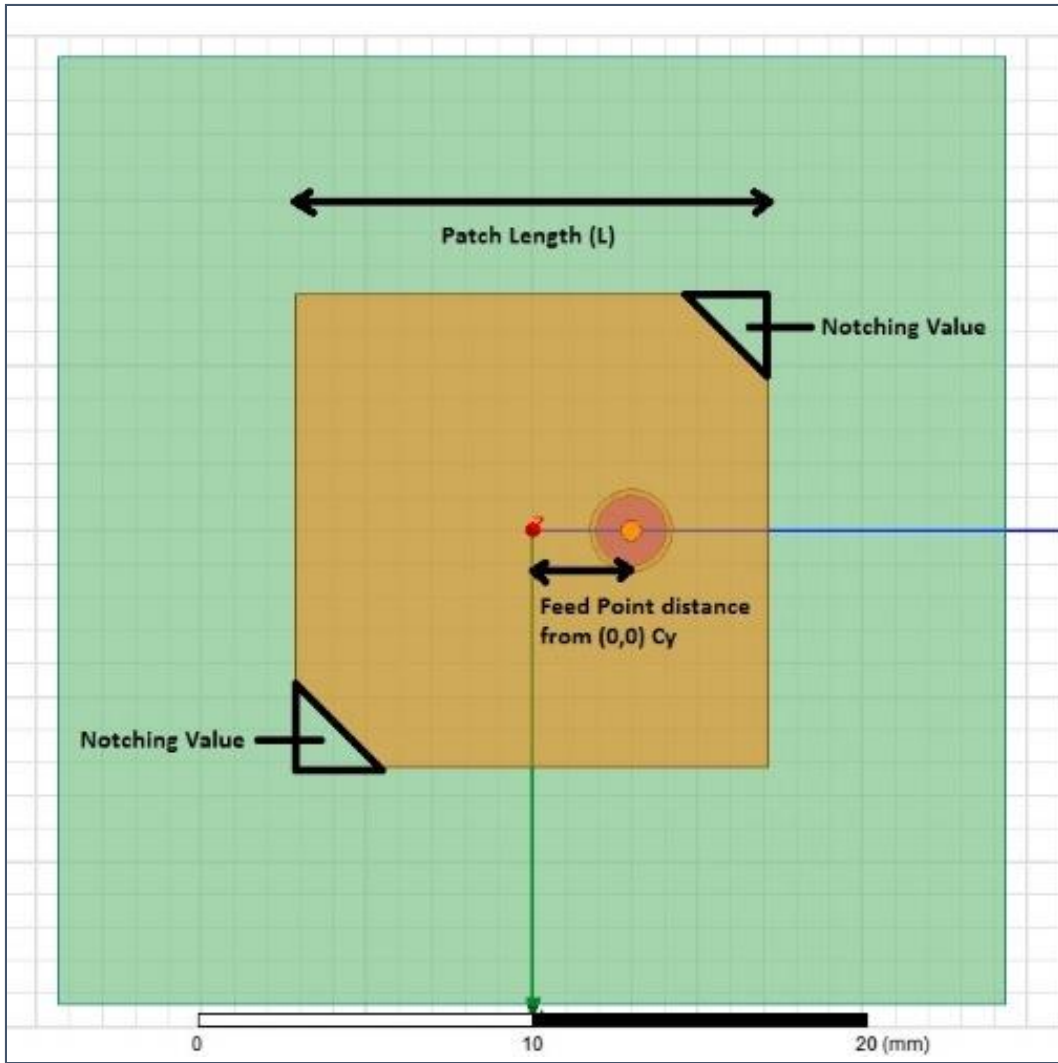


Fig. 6 Transverse plane (XY plane) of patch

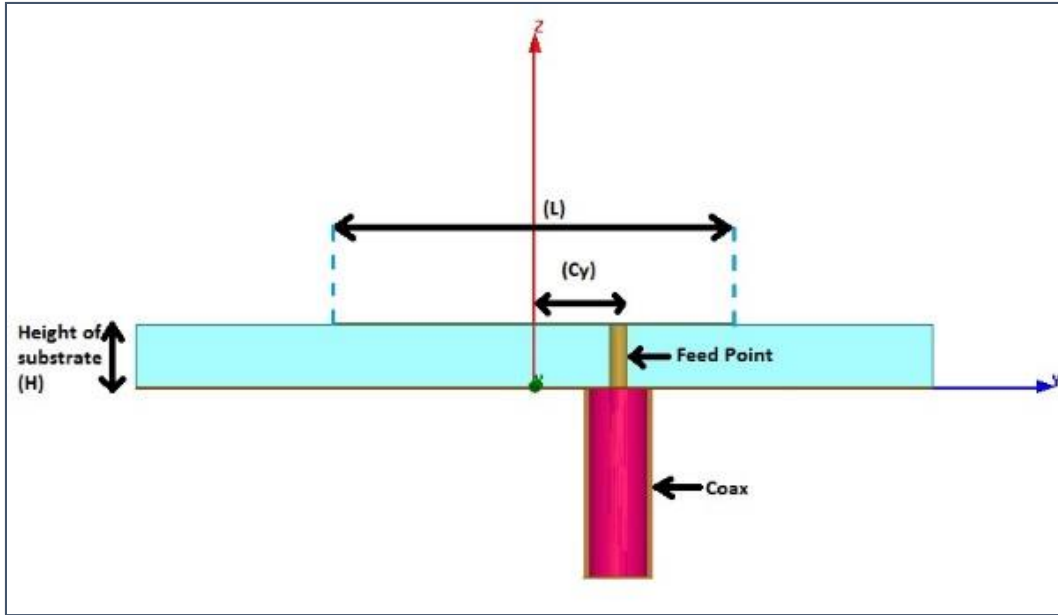


Fig. 7 Normal (YZ) plane of patch antenna

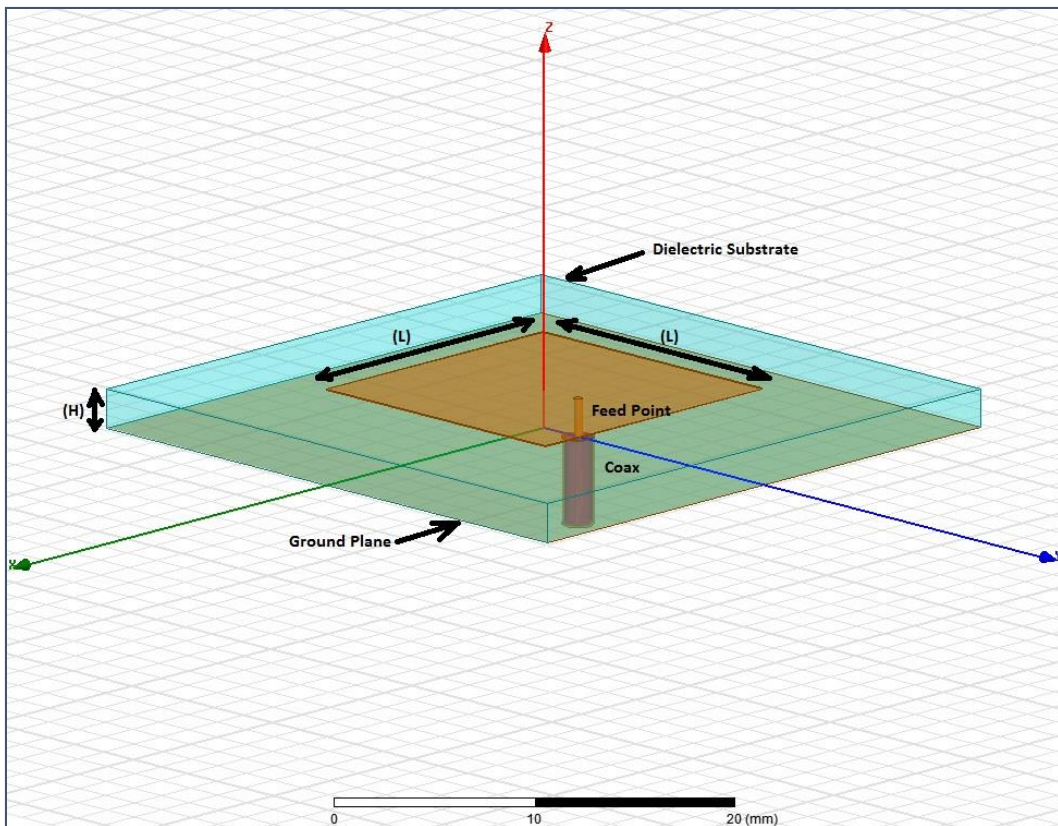


Fig. 8 HFSS patch antenna model, 3-dimensional view

Table 1 Variable list for Rogers 5870

Name	Description	Value/Unit
L	Length of Patch Antenna	10.5 mm
Cx	X-direction of coax	0
Cy	Y-direction of coax	0
Cz	Z-direction of coax	0
H	Height of dielectric	1.5 mm
NV	Notching Value	0

Table 2 Variable list for Rogers 6010

Name	Description	Value/Unit
L	Length of Patch Antenna	16.5 mm
Cx	X-direction of coax	0
Cy	Y-direction of coax	0
Cz	Z-direction of coax	0
h	Height of dielectric	2 mm
NV	Notching Value	0

2.1 Patch on Rogers 5870

We wanted the X-band element to radiate at 9.35 GHz on the Rogers 5870 material. As a result, the patch length was calculated as follows

$$\lambda = \frac{c \text{ (Speed of Light)}}{f * (\sqrt{\epsilon_r \mu_r})} = \frac{3 * 10^8}{(9.35 * 10^9) * (\sqrt{2.33})} \approx 0.021 \text{ m};$$

$$L = \frac{\lambda}{2} = \frac{0.021}{2} \approx \mathbf{10.5 \text{ mm}}$$

Table 1 displays the variables used to design the antenna to verify the HFSS simulation setup.

The feed point was swept from the center of the patch (0,0,0) to the outer edge (0,3.2,0) to locate the position at which the patch resonated best. As shown in Fig. 9, the S11 plot shows that the best curve corresponds to a 9.26-GHz frequency with a -25.71-dB null. This occurs when the probe is 2 mm away from the center position of the patch, as shown in Fig. 10.

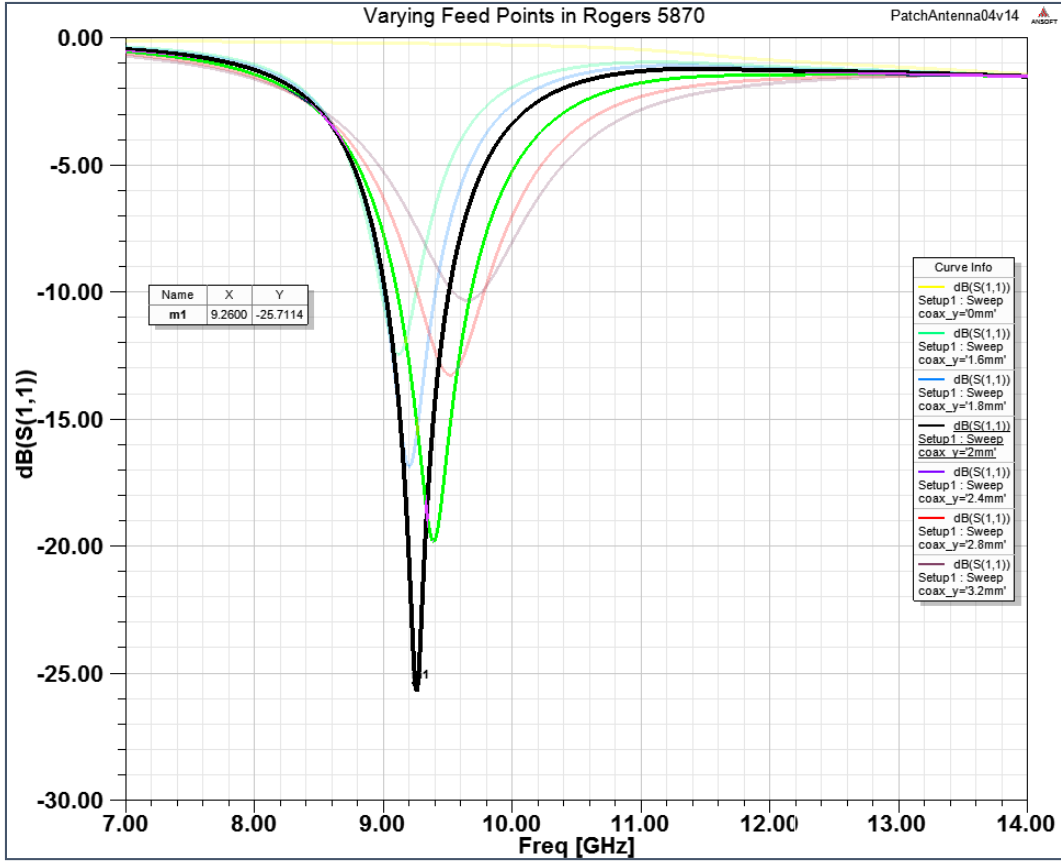


Fig. 9 Return loss for varying feed points in Rogers 5870. Best S11 curve corresponds to $C_y = 2$ mm.

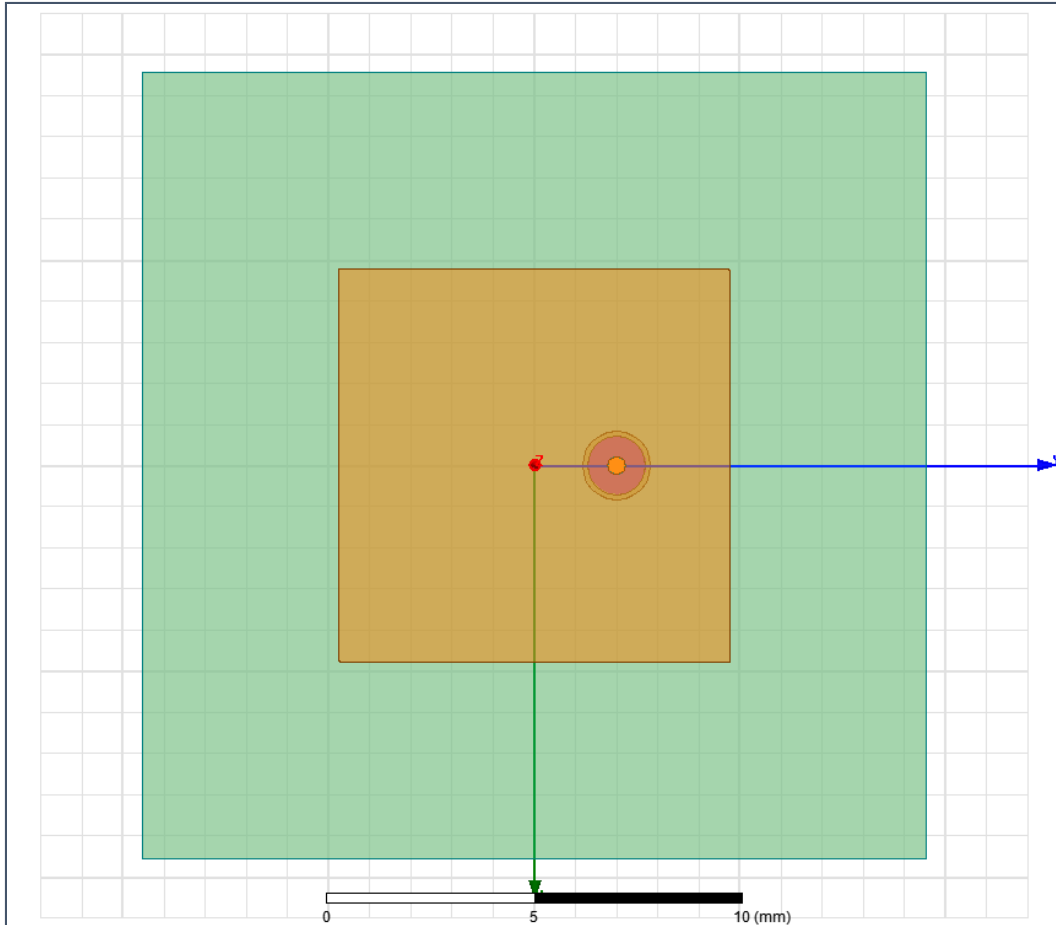


Fig. 10 Probe 2 mm away from center position, which corresponds to a 9.26-GHz frequency

Next, the notching technique was implemented by trimming opposite corners of the patch. A parameter sweep was performed on HFSS from a 0.36 to 0.51 SF. As shown in Fig. 11, the best S11 curve is found when the scaling factor was equal to 0.46 resulting in a notching value of 2.83 mm shown in Fig. 12.

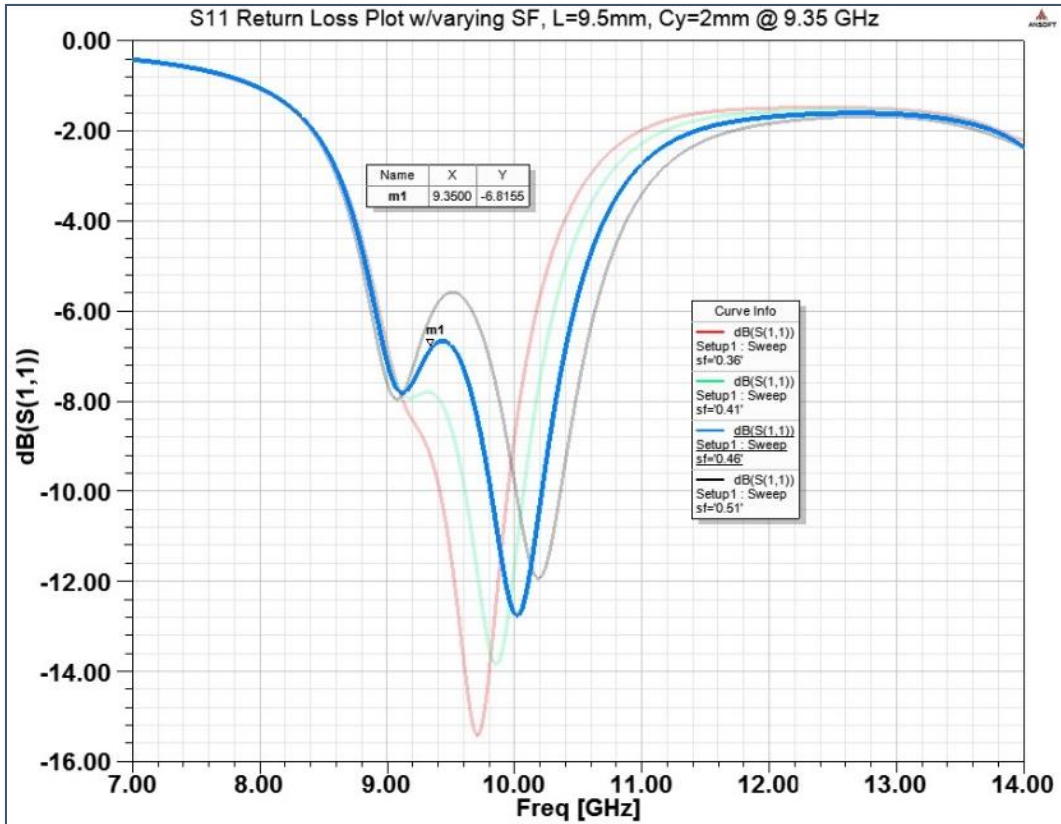


Fig. 11 Return loss for varying SF in Rogers 5870

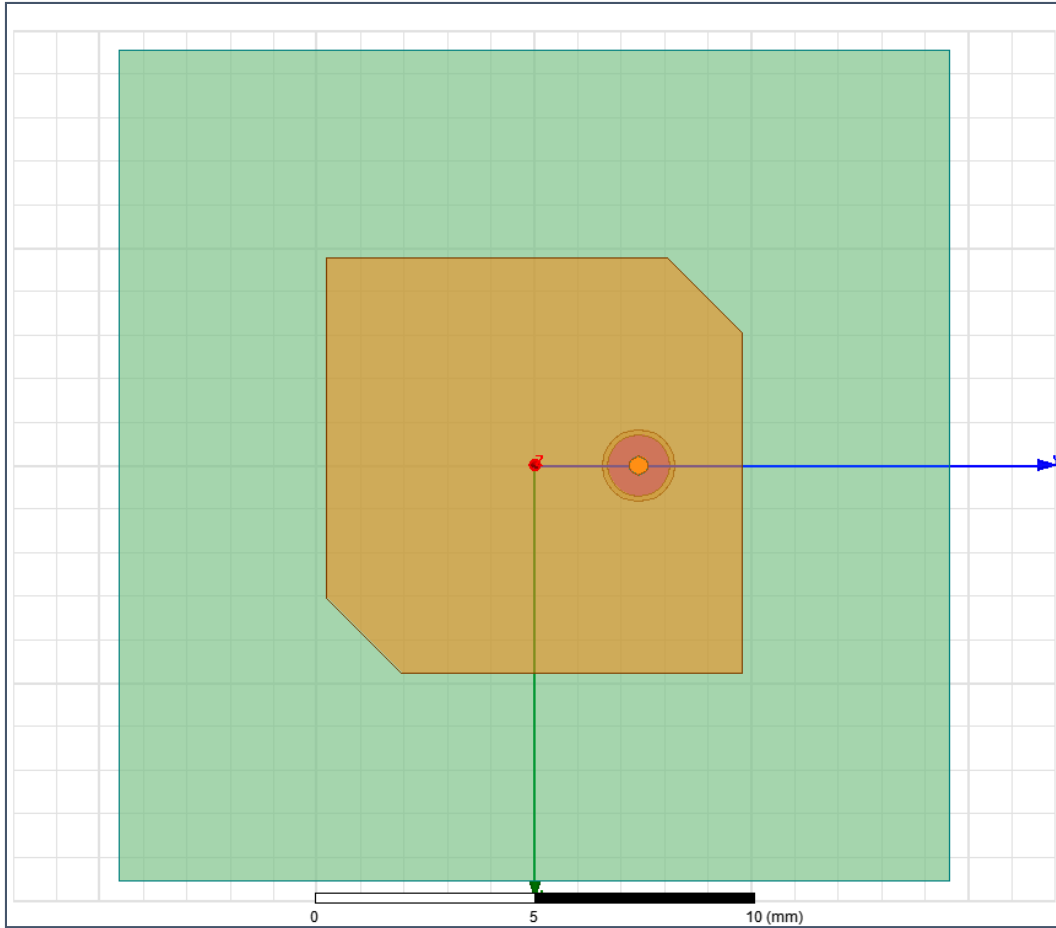


Fig. 12 SF = 0.46 on Rogers 5870 substrate with feed point 2 mm from center position

After finding the best SF to notch the patch, an axial ratio calculation was performed, as shown in Fig. 13. With the coax probe 2 mm away from the center of the patch, the best SF value of 0.46 corresponds to 9.35 GHz with an optimal axial ratio at 1.11 dB.

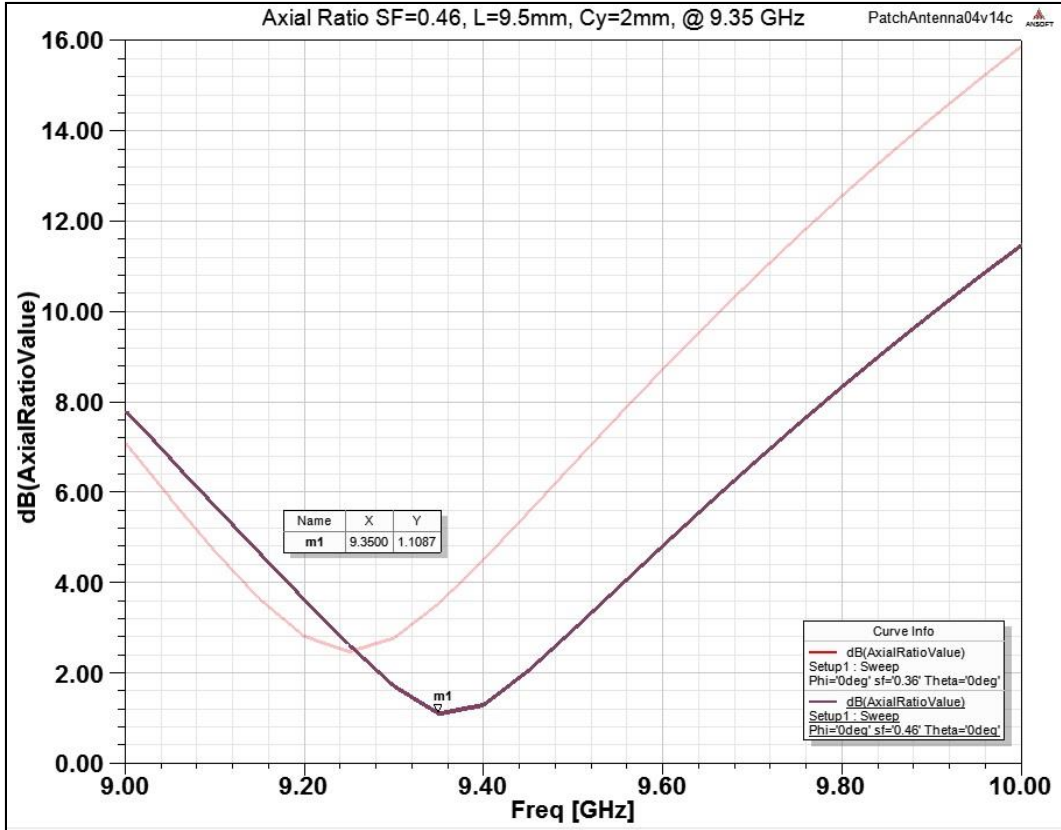


Fig. 13 Axial ratio for the best SF—corresponds to 9.35 GHz with an optimal axial ratio of 1.11 dB

Lastly, the realized gain was calculated to confirm the S11 curves and axial ratio results as shown in Fig. 14. The patch experienced a 6.19 dB peak realized gain to boresight at 9.35 GHz for optimal axial ratio.

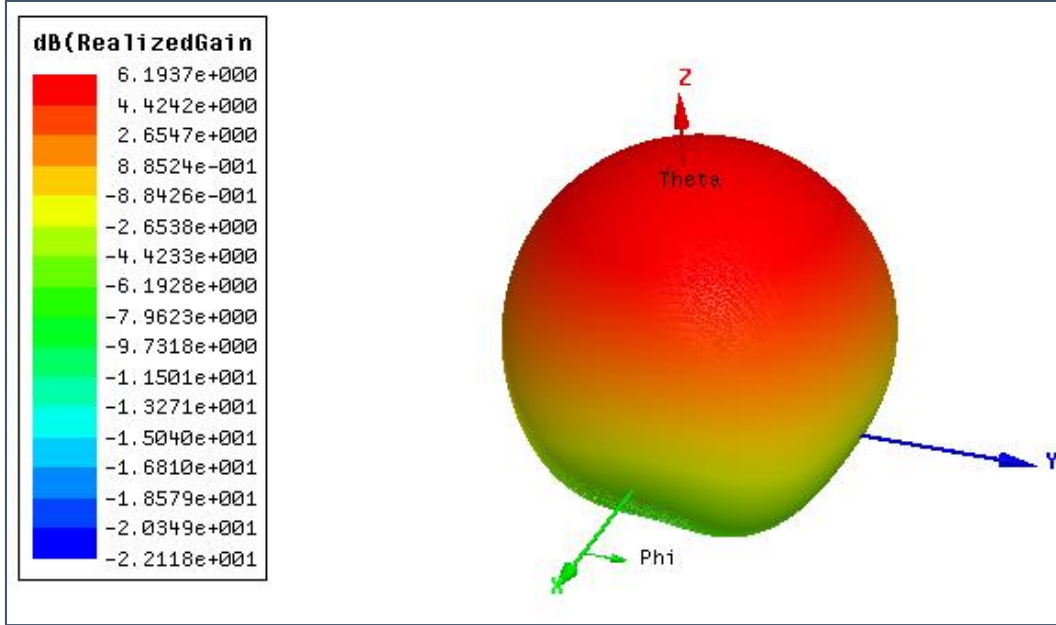


Fig. 14 Radiation plot at 9.35 GHz for optimal axial ratio. Boresight pattern with a 6.19-dB gain.

2.2 Patch Rogers 6010

We wanted the S-band element to radiate at 2.83 GHz. The calculations below show the length of the patch if the S-band patch was placed on the Rogers 5870:

$$\lambda = \frac{c \text{ (Speed of Light)}}{f * (\sqrt{\epsilon_r \mu_r})} = \frac{3 * 10^8}{(2.83 * 10^9) * (\sqrt{2.33})} \approx 0.069 \text{ m};$$

$$L = \frac{\lambda}{2} = \frac{0.069}{2} \approx \mathbf{34.7 \text{ mm}}$$

We can see that the S-band patch shrinks by approximately 18.2 mm or 52.4% by placing it on the Rogers 6010 substrate instead per the calculations below:

$$\lambda = \frac{c \text{ (Speed of Light)}}{f * (\sqrt{\epsilon_r \mu_r})} = \frac{3 * 10^8}{(2.83 * 10^9) * (\sqrt{10.2})} \approx 0.033 \text{ m};$$

$$L = \frac{\lambda}{2} = \frac{0.033}{2} \approx \mathbf{16.5 \text{ mm}}$$

The feed point was swept from the center of the patch (0,0,0) to the outer edge (0,7.2,0) to locate the position at which the patch resonated best. As shown in Fig. 15, the S11 plot shows that the best curve corresponds to a 2.83-GHz frequency with a -12.76-dB null. This occurs when the probe is 2.4 mm away from the center position of the patch, as shown in Fig. 16.

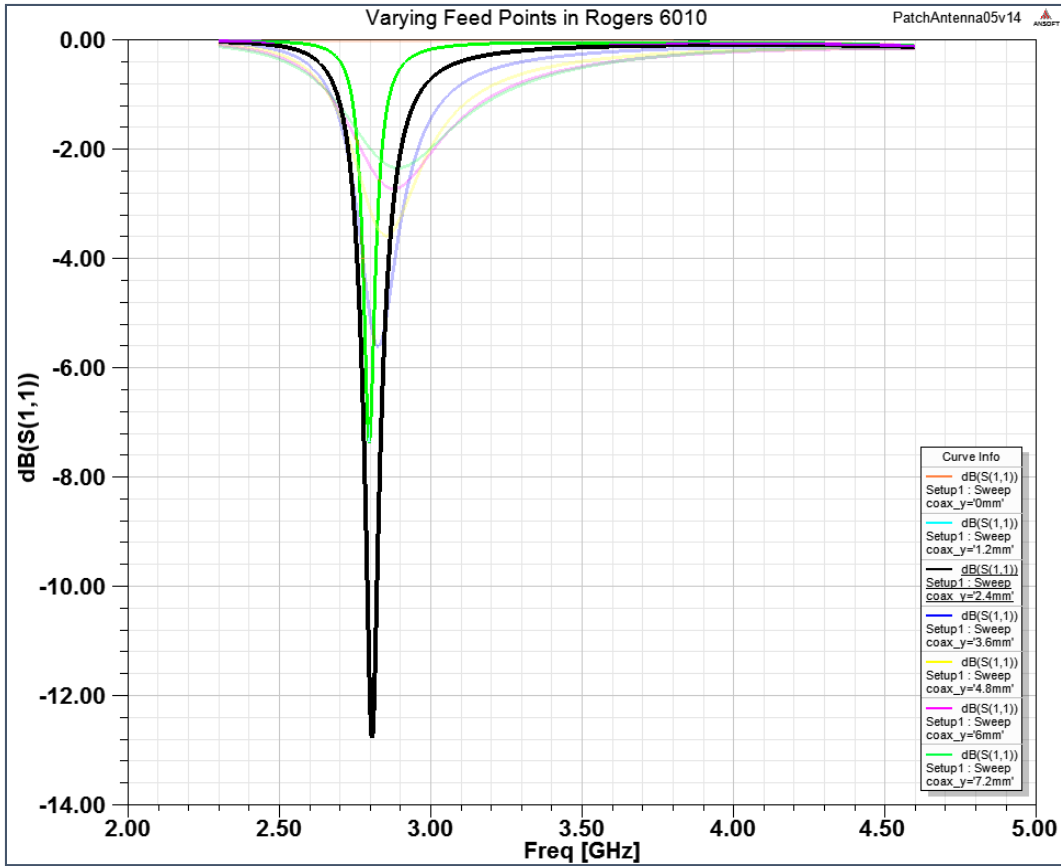


Fig. 15 Return loss for varying feed points in Rogers 6010. Best S11 curve corresponds to $C_y=2.4$ mm.

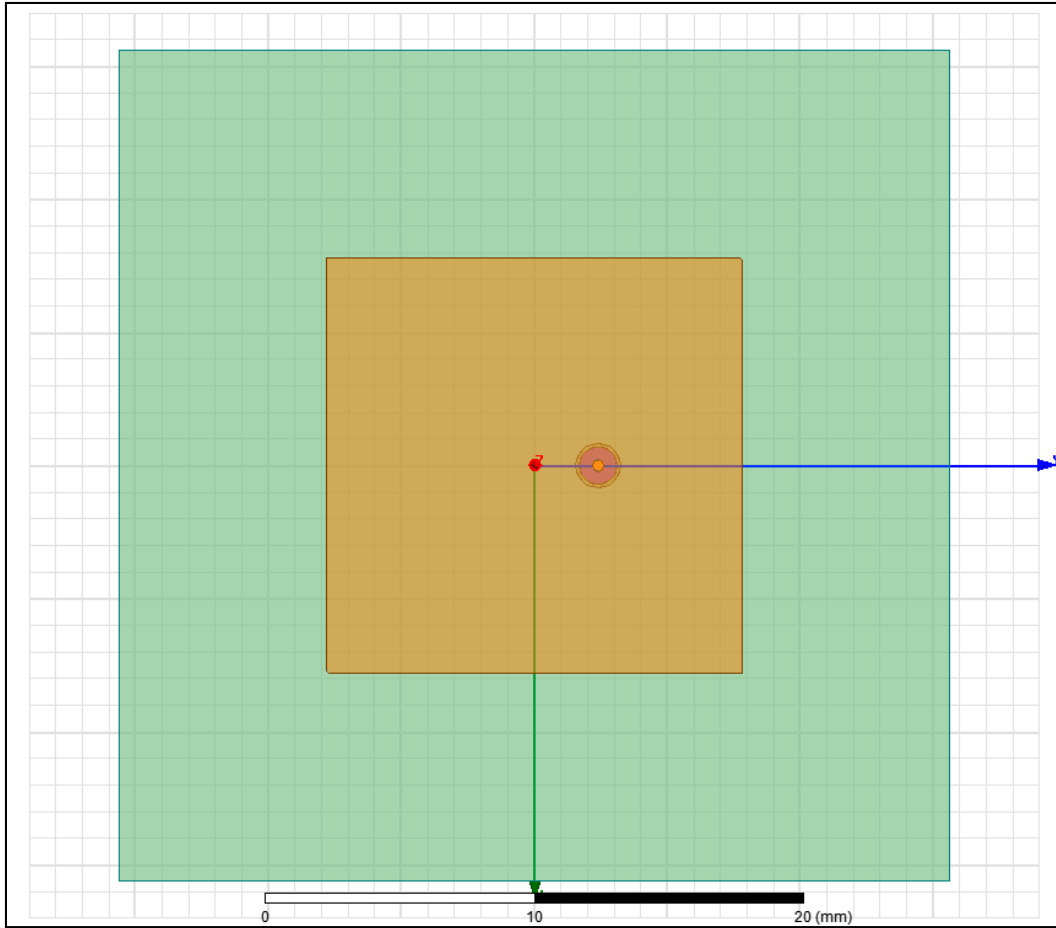


Fig. 16 Probe 2.4 mm away from center position, which corresponds to a 2.83-GHz frequency

As performed on the Rogers 5870, the notching technique was implemented by trimming the opposite corners of the patch. A parameter sweep was performed on HFSS of a 0.01 to a 1.11 SF. As shown in Fig. 17, the best S11 curve is found when SF was equal to 0.21 resulting in a notching value of 6.52 mm as shown in Fig. 18.

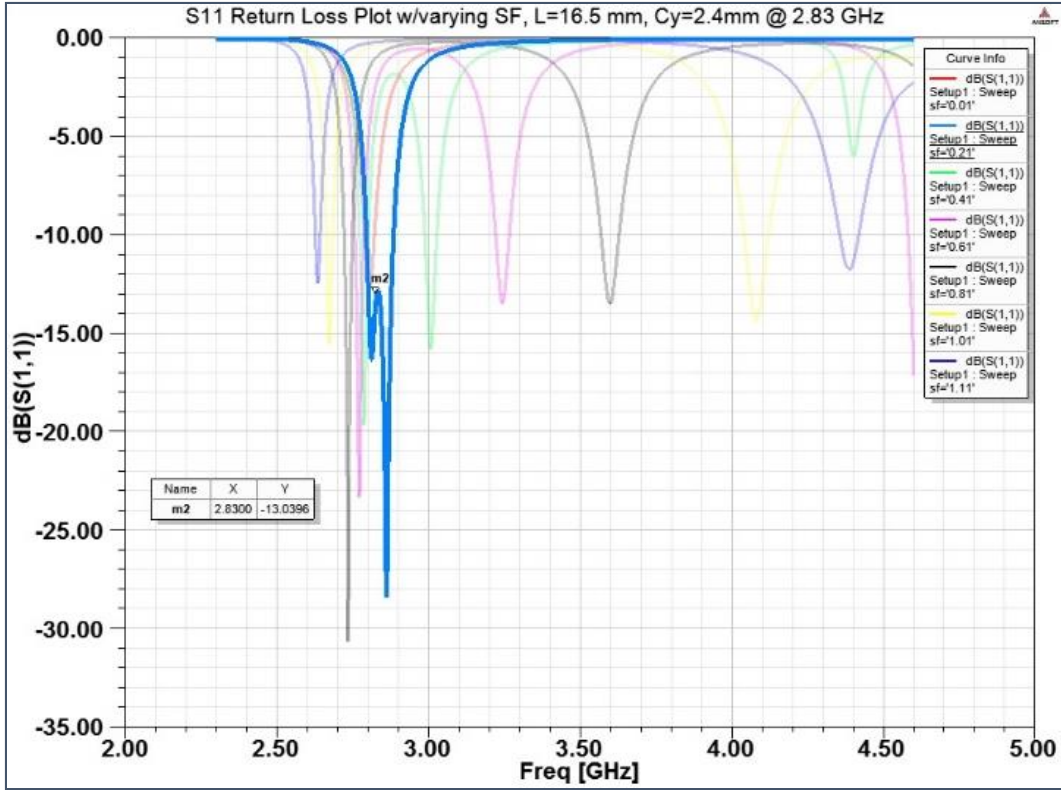


Fig. 17 Return loss for varying SF in Rogers 6010

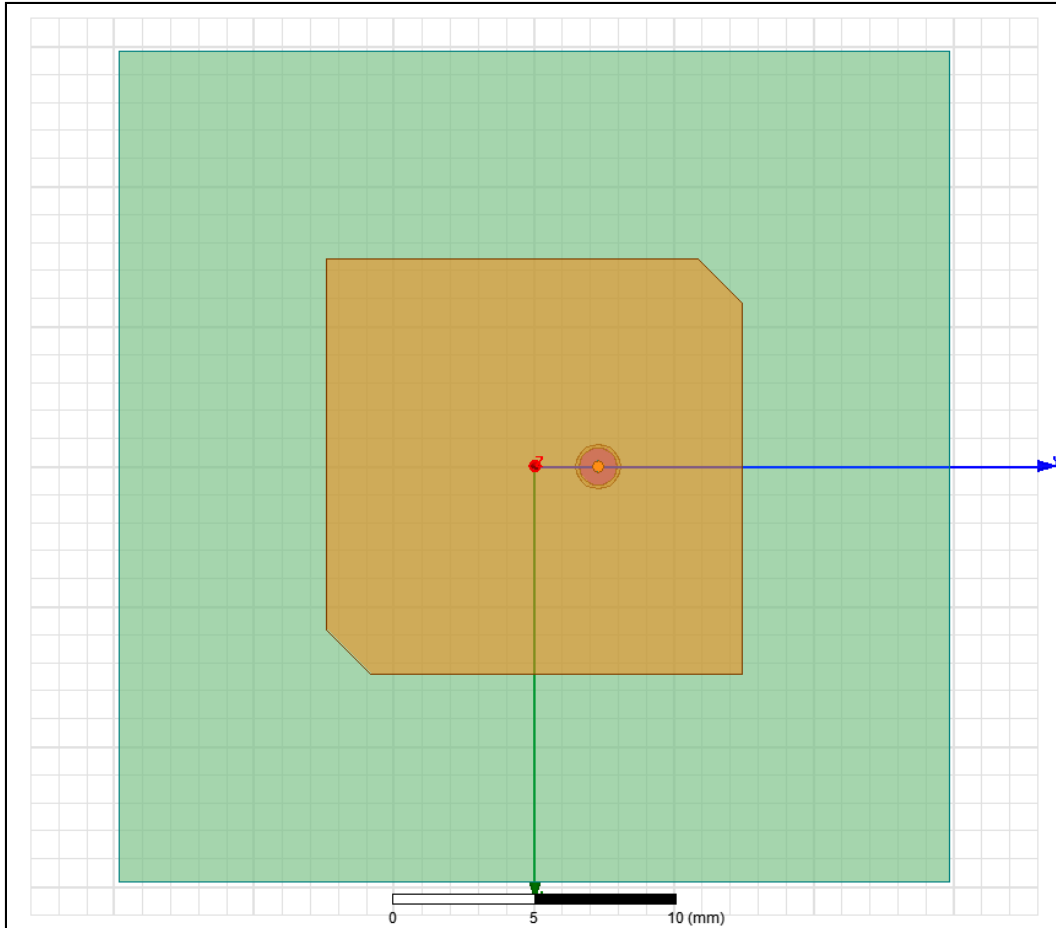


Fig. 18 SF = 0.21 on Rogers 6010 substrate with feed point 2.4 mm from center position

After executing the axial ratio test as shown in Fig. 19, it was found that the SF=0.21 corresponds to 2.83 GHz with an optimal axial ratio of 1.61 dB.

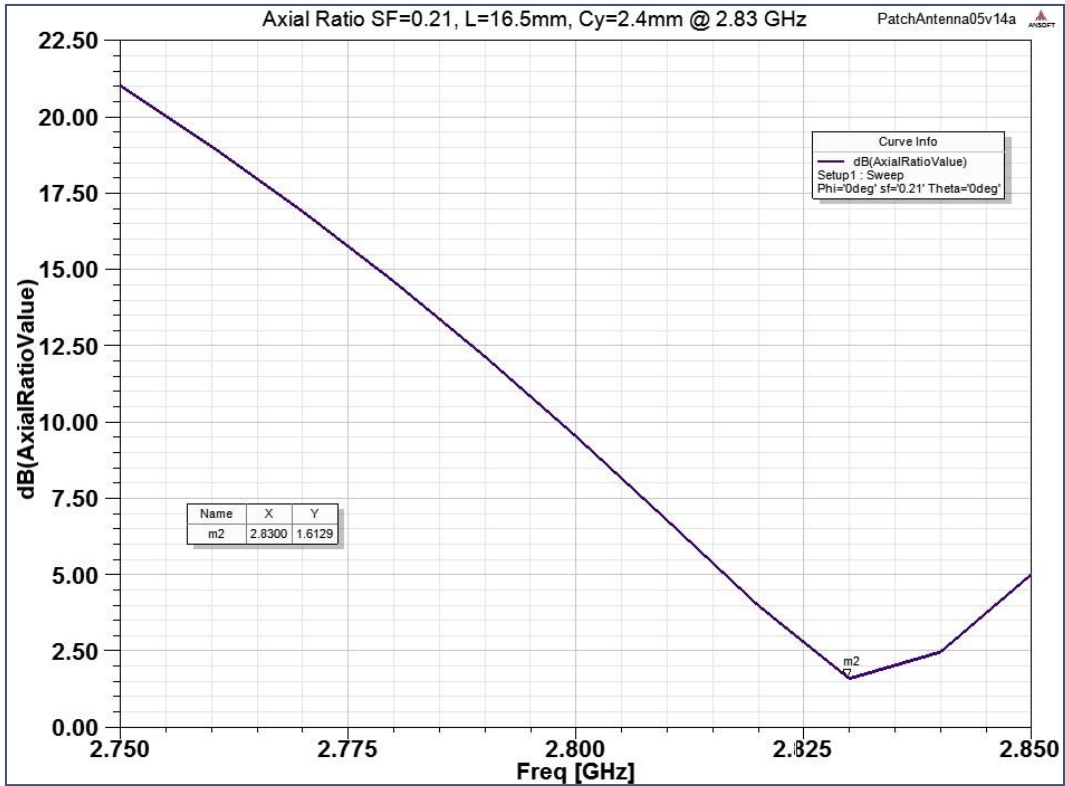


Fig. 19 Rogers 6010 axial ratio for the best SF—corresponds to 2.83 GHz with an optimal axial ratio of 1.61 dB

Figure 20 exhibits that the patch containing the Rogers 6010 substrate experiences a 4.62-dB peak realized gain to boresight at 2.83 GHz for optimal axial ratio.

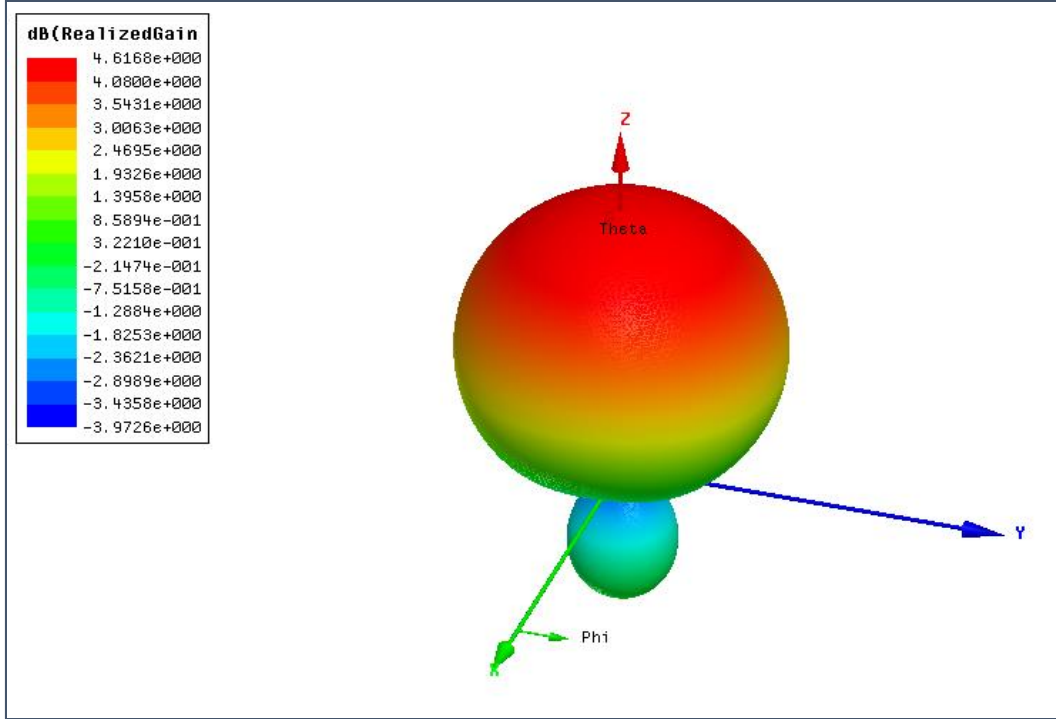


Fig. 20 Rogers 6010 radiation plot at 2.83 GHz for optimal axial ratio. Boresight pattern with a 4.62-dB gain.

3. Results and Discussion

We were able to effectively obtain an optimal impedance match, axial ratio, and realized gain for 2 antennas designed at 2 frequency bands on 2 different substrates. Testing the feed point in various locations on the patch allows the designer to improve the S11 and radiation pattern. The best return loss does not necessarily correspond to the best axial ratio, therefore, the engineer must account for the tradeoffs in S11, axial ratio, and the radiation pattern.

A dielectric with high permittivity lowers the resonant frequency of the patch, allowing the designer to shrink the size of the patch. We were able to shrink the size of the S-band patch by 52.4% due to placing it on a Rogers 6010 substrate instead of a Rogers 5870 substrate. Optimizing the axial ratio by using a “notching” technique allows the antenna to achieve CP with a single feed point.

4. Future Work

We wish to demonstrate that we can combine a high frequency and low frequency elements in the same antenna for dual-band performance. We believe that combining a high frequency and low frequency element in the same antenna for

dual-band performance will be an agile, adaptable, and cost-effective solution for future US Army Research Laboratory (ARL) projects. Figures 21 and 22 show the envisioned geometry of such an antenna. This antenna would achieve both right-hand CP (RHCP) and left-hand CP (LHCP) at 2 frequency bands.

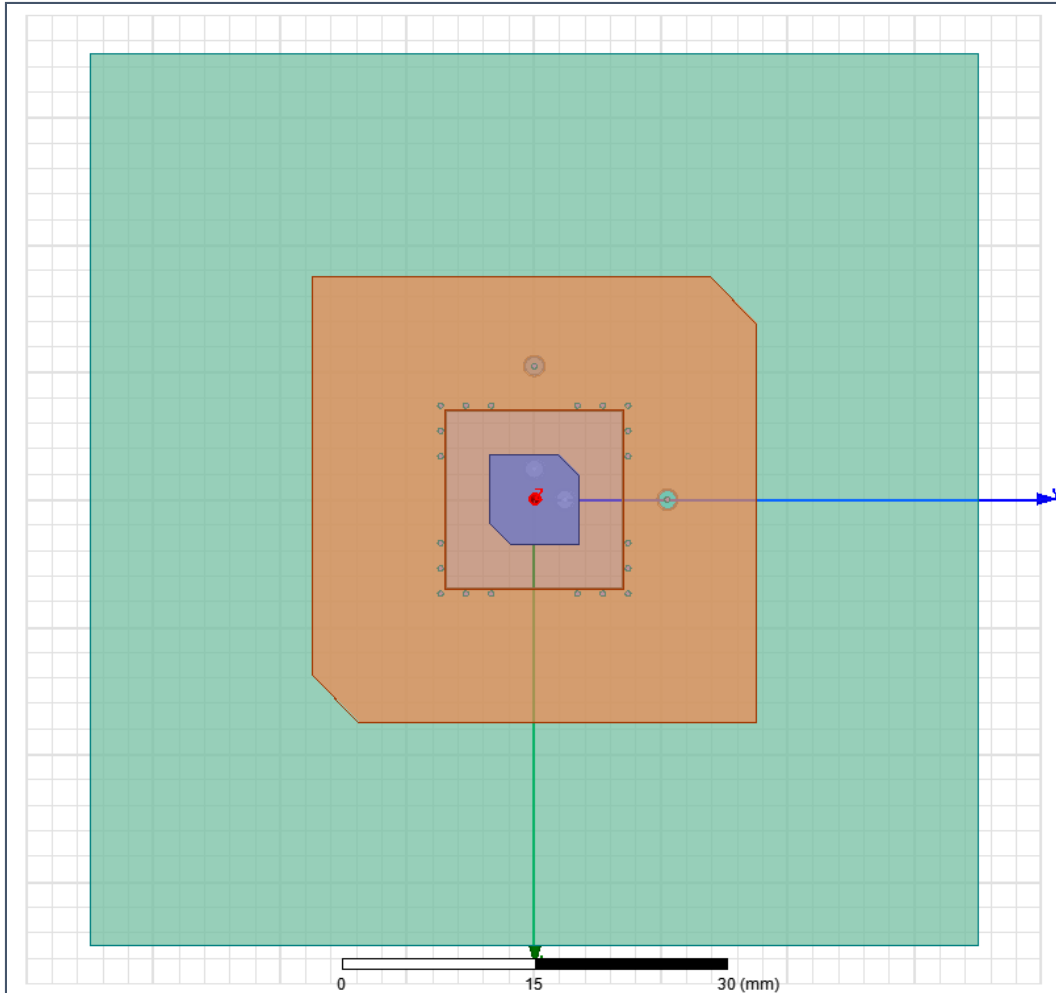


Fig. 21 Transverse (XY) plane of the proposed dual-band antenna design

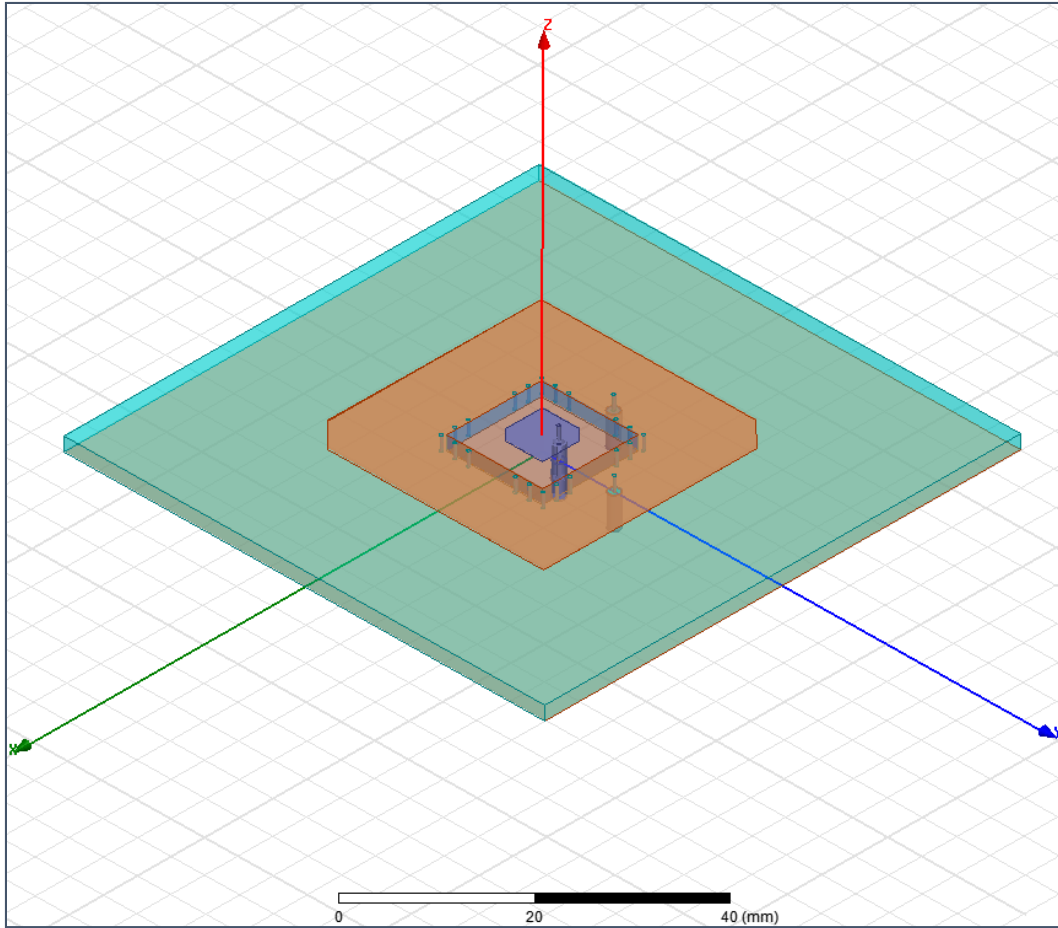


Fig. 22 HFSS model of the dual-band antenna, 3-dimensional view

5. References

1. Breed G. The fundamentals of patch antenna design and performance. High Frequency Electronics and Patch Antennas, Summit Technical Media, LLC, 2009.
2. Balanis C. Microstrip antenna. Antenna Theory, John Wiley & Sons Inc., 2005.
3. Frenzel L. What's the difference between a dipole and a ground plane antenna? Electronic Design, July 2013. <http://electronicdesign.com/wireless/what-s-difference-between-dipole-and-ground-plane-antenna>.

- 1 DEFENSE TECH INFO CTR
(PDF) DTIC OCA
- 2 US ARMY RSRCH LAB
(PDF) IMAL HRA MAIL & RECORDS MGMT
RDRL CIO LL TECHL LIB
- 1 GOVT PRNTG OFC
(PDF) A MALHOTRA
- 5 US ARMY RSRCH LAB
(PDF) RDRL SER M
G MITCHELL
A ZAGHLOUL
T ANTHONY
S WEISS
E ADLER